Title

Contribution of hydraulically lifted deep moisture to the water budget in a Southern California mixed forest

Journal

Journal of Geophysical Research Biogeosciences, 118(4)

ISSN

2169-8953

Authors

Kitajima, Kuni
Allen, Michael F
Goulden, Michael L

Publication Date

2013-12-01

DOI

10.1002/2012jg002255

JOURNAL OF GEOPHYSICAL RESEARCH: BIOGEOSCIENCES, VOL. 118, 1561–1572, doi:10.1002/2012JG002255, 2013

Contribution of hydraulically lifted deep moisture to the water budget in a Southern California mixed forest

Kuni Kitajima,[1] Michael F. Allen,[1] and Michael L. Goulden[2]

Received 3 December 2012; revised 15 October 2013; accepted 18 October 2013; published 25 November 2013.

[1] Trees and shrubs growing in California's mountains rely on deep roots to survive the hot and dry Mediterranean climate summer. The shallow montane soil cannot hold enough water to support summer transpiration, and plants must access deeper moisture from the weathered bedrock. We used the HYDRUS-1D model to simulate the moisture flux through the soil-plant continuum in Southern California's San Jacinto Mountains. The mechanisms facilitating deep water access are poorly understood, and it is possible that either or both hydraulic lift and capillary rise contribute to the survival and activity of trees and soil microorganisms. We modified HYDRUS to incorporate hydraulic lift and drove it with meteorological and physiological data. The modeled quantity of water lifted hydraulically ranged from near zero during the wet months to ~28 mm month^{-1} in midsummer. Likewise, modeled capillary rise was negligible during the winter and averaged ~15 mm month^{-1} during June through November. Both mechanisms provided water to support evapotranspiration during the dry months. Isotopic measurements of xylem water for eight shrub and tree species confirmed the importance of a deep source of water. Conventional and automated minirhizotron observations showed that fine-root and rhizomorph biomass remained relatively constant year-round, while mycorrhizal hyphae biomass varied markedly, peaking in the wet season and declining by ~70% in the dry season. Model results predict that hydraulic lift and capillary rise play key roles in Southern California's mountains: they support evapotranspiration and photosynthesis during the summer drought; they contribute to the year-round survival of fine roots and soil microorganisms.

Citation: Kitajima, K., M. F. Allen, and M. L. Goulden (2013), Contribution of hydraulically lifted deep moisture to the water budget in a Southern California mixed forest, *J. Geophys. Res. Biogeosci.*, *118*, 1561–1572, doi:10.1002/2012JG002255.

1. Introduction

[2] Southern California's mountains rise above 3000 m, creating strong orographic precipitation gradients and a montane Mediterranean climate. The resulting mosaic of evergreen and deciduous hardwood and conifer forest is a biodiversity hotspot. Precipitation arrives during the cool winter as a mix of snow and rain; the summer is hot and dry with very infrequent monsoonal rains. Mean precipitation is low and exceedingly variable, averaging 665 mm yr^{-1} (1982–2010) on the west slope of the San Jacinto Mountains. The soils are shallow entisols overlying weathered granitic regolith and bedrock. Water storage in the surface soil is inadequate to sustain plant growth through the summer and fall, and trees and shrubs rely on water from the weathered granite for survival [*Hubbert et al.*, 2001; *Witty et al.*, 2003; *Ichii et al.*, 2009; *Graham et al.*, 2010; *Bales et al.*, 2011]. Climate models project 3°C to 5°C warming in inland Southern California by 2100, which will increase both thermal stress and potential evapotranspiration [*Hayhoe et al.*, 2004; *Cayan et al.*, 2008]. Moreover, precipitation variability is expected to increase, and the snow to rain transition is expected to rise, leading to long droughts punctuated by heavy rains, as opposed to the slower input of water during snowmelt that has been common over the last century. The future of these forests will likely depend on plant access to deep water; a more quantitative understanding of the input, redistribution, and withdrawal of water within these ecosystems is needed to project and manage the impact of climate change.

[3] Evergreen Mediterranean climate plants often tap deep water during the dry season [e.g., *Hubbert et al.*, 2001; *Warren et al.*, 2007; *Querejeta et al.*, 2007, 2009; *Miller et al.*, 2010; *Orellana et al.*, 2012]. Three mechanisms may mediate plant access to deep moisture. First, water may move upward through small soil and rock pores by capillary rise driven by large water potential gradients [e.g., *Bales et al.*, 2011; *Glenn et al.*, 2012]. Second, moisture may be drawn into deep roots and directly transported to the canopy for transpiration [e.g., *Ichii et al.*, 2009; *Miller et al.*, 2010]. Third, moisture may be drawn into deep roots and subsequently "lifted"

Additional supporting information may be found in the online version of this article.

[1]Center for Conservation Biology, University of California, Riverside, California, USA.
[2]Department of Earth System Science, University of California, Irvine, California, USA.

Corresponding author: K. Kitajima, Center for Conservation Biology, University of California, Riverside, CA 92521-0334, USA. (kunik@ucr.edu)

2169-8953/13/10.1002/2012JG002255

or "redistributed" to shallow horizons, where it passively flows to the soil through fine roots and hyphae [e.g., *Richards and Caldwell*, 1987; *Ludwig et al*., 2003; *Querejeta et al*., 2003; *Kurz-Besson et al*., 2006; *Egerton-Warburton et al*., 2008; *Warren et al*., 2008; *Prieto et al*., 2012]. Broader forms of plant-mediated hydraulic redistribution are also possible, including vertical or horizontal water movement and upward or downward transport.

[4] Trees and shrubs in Mediterranean climate ecosystems rely heavily on symbiotic fungal relationships for nutrient and water uptake [e.g., *Allen*, 1991; *Allen et al*., 2003]. Mycorrhizal hyphae extend into the weathered granite matrix and very fine saprock microfractures (in a broad sense *Graham et al*. [2010]), thereby facilitating deep water uptake [*Egerton-Warburton et al*., 2003; *Bornyasz et al*., 2005]. Mycorrhizal root tips may persist for years or decades by tolerating freezing, thawing, drought, and rewetting [*Allen*, 1991; *Ruess et al*., 2003; *Allen et al*., 2003]. Laboratory studies have shown that the water provided through hydraulic lift contributes to the survival of mycorrhizal hyphae [*Querejeta et al*., 2003] and associated shallowly rooted seedlings [*Egerton-Warburton et al*., 2007] and also facilitates N uptake [*Egerton-Warburton et al*., 2008]. California evergreen oaks redistribute deep water to the surface, which is thought to sustain ectomycorrhize through the dry season [*Querejeta et al*., 2009]. Similarly, isotopic analyses have shown that seedlings in the field receive deep water through mycorrhizal connections [*Querejeta et al*., 2003]. Ectomycorrhizal sporocarp production can continue despite extreme drought and inadequate surface water availability [*Allen*, 2009]; sporocarps may utilize hydraulically lifted water for growth [*Lilleskov et al*., 2009].

[5] A range of experimental approaches are available for measuring in situ water dynamics, including sap flow sensors, which can be installed in tap or lateral roots [*Burgess et al*., 1998; *Nadezhdina et al*., 2010], and also amended or natural abundance isotopic tracers [*Moreira et al*., 2003; *Kurz-Besson et al*., 2006; *Querejeta et al*., 2009]. The isotopic composition of moisture in the weathered bedrock is usually similar to that of the local precipitation, while the composition of moisture in the surface soil is shifted by evaporative fractionation. The isotopic composition of water extracted from a plant therefore provides a measure of water source. Similarly, a range of models are available for simulating water, carbon, and nutrient cycles, including (the daily version of the CENTURY ecosystem model) [*Parton et al*., 1998], CENTURY [*Parton et al*., 1993], PnET (simple, lumped-parameter, monthly-time-step model of carbon and water balances of forests) [*Aber and Federer*, 1992], SIPNET (the simplified Photosynthesis and Evapo-Transpiration model) [*Braswell et al*., 2005], HYDRUS-1D [*Simunek et al*., 2005], and many others [e.g., *Amthor et al*., 2001; *Tang et al*., 2006; *Knohl and Baldocchi*, 2008].

[6] We combined observations and modeling to investigate the moisture flux through the soil-plant continuum at the James Reserve in Southern California's San Jacinto Mountains. We collected climate, belowground microclimate, plant physiological, plant biomass, root and rhizomorph, and stable isotopic data over a 7 year period. We used these data to calibrate and refine the HYDRUS-1D model (available at http://www.pc-progress.com/en/Default.aspx?hydrus-1d). HYDRUS has been used successfully to address problems in ecology, environmental science, soil science, and agriculture [e.g., *Yin et al*., 2008; *Yuan et al*., 2011]. HYDRUS was configured to predict evapotranspiration, plant water uptake (sap flow density), soil CO_2 efflux, soil temperature, soil water content, and CO_2 concentration. Our specific objectives are to (1) develop, calibrate, and validate a model to simulate water and CO_2 flux, (2) refine the model to incorporate hydraulic lift, (3) estimate how much water is hydraulically lifted to the surface layer and how it varies seasonally, and (4) infer whether lifted water contributes to the survival of mycorrhizal fungi.

2. Methods

2.1. Study Site

[7] Observations were made at the University of California James Reserve (http://www.jamesreserve.edu) located in the San Jacinto Mountains in Riverside County, California, USA (Elevation: 1650 m, Longitude: 33.8078°N, Latitude: 116.7771°W). The site is an old-growth, uneven-aged, mixed-conifer forest. Dominant trees include ponderosa pine (*Pinus ponderosa* C. Lawson), sugar pine (*P. lambertiana* Douglas), incense cedar (*Calocedrus decurrens* (Torr.) Florin), and canyon live oak (*Quercus chrysolepis* Liebm.), which are all evergreen, and black oak (*Q. kelloggii* Newberry), which is winter deciduous. Manzanita (*Arctostaphylos glandulosa* Eastw.) is the dominant understory shrub, and there are scattered herbs and grasses. The climate is montane Mediterranean with cool, wet winters and hot, dry summers. Daily average air temperature ranges from −5°C in winter to 23°C in summer. Most of the precipitation falls during the winter; very occasional and highly variable monsoonal rains fall during the summer. Soils are shallow (~2 m) sandy loams belonging to the Pacifico-Wapi, Pacifico-Preston, and Green Bluff-Brader families (http://websoilsurvey.nrcs.usda.gov).

2.2. Field Observations

[8] Most of our measurements were made along a gently sloping 76 m transect (<10°, Figure S1 in the supporting information). We began meteorological observations at the transect in 2000 (air temperature, relative humidity, solar radiation, wind direction and speed, and precipitation; ONSET®, U30-NRC-000-10-S045-000). We added observations of soil conditions at 10 nodes along the transect in 2005; soil temperature (ONSET® S-TMB-M002), moisture (ONSET®, S-SMC-M005), and CO_2 concentration (Vaisala®, GMM222F0N0A4A2E1B) were recorded every 5 to 15 min at three depths (0.02, 0.08, and 0.16 m).

[9] Sap flow was recorded every 30 min with thermal dissipation probes (Dynamax®, FLGS-TDP XM1000, and TDP-30) on three dominant tree species (ponderosa pine, sugar pine, and black oak). Two to six 30 mm long probes were inserted into the sapwood of each tree (21 probes total). The probes were insulated with two or more layers of reflective foil insulation (2 ft wide × 1/4 in thick) to reduce thermal gradients. The sap flow (mm d^{-1}) was calculated using Granier's formula [*Granier*, 1987]:

$$\text{Sap flow rate} = 119*3600*24*10^{-3}*[(\Delta DT_{\max} - \Delta DT)/\Delta DT]^{1.231},$$

where, ΔT is the temperature difference between the heated and reference probes and ΔT_{max} is the ΔT at zero sap flow.

[10] Fine-root/rhizomorph growth was monitored weekly beginning in 2005 with 15 conventional minirhizotron

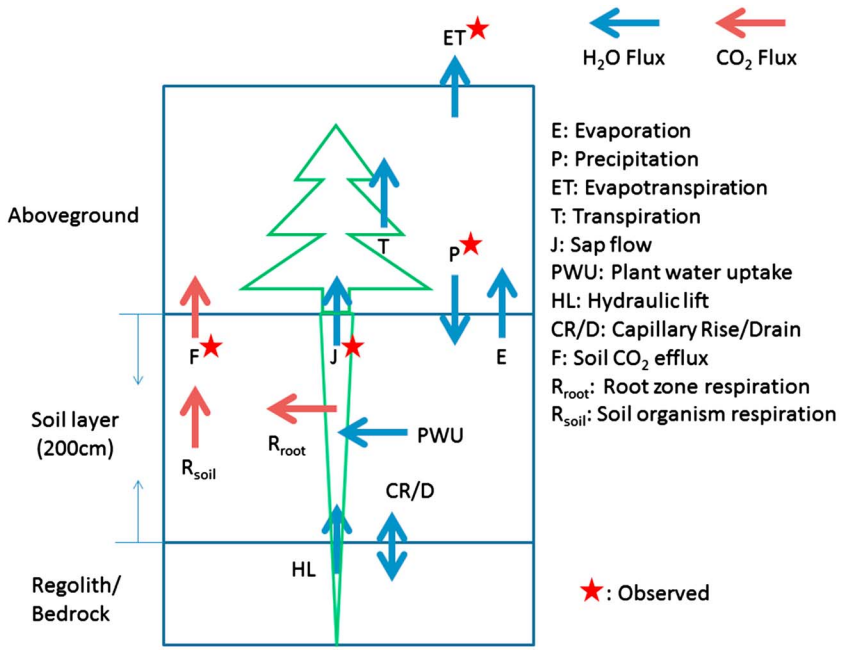

Figure 1. Schematic of observed and estimated fluxes. Fluxes marked with a red star were observed; unmarked were estimated with the model. The direction of arrow shows the positive value of the flow. Actual fluxes flow both ways.

(CMR) tubes and a Bartz minirhizotron (Bartz Technology®, Santa Barbara, CA) [*Allen et al.*, 2007; *Vargas and Allen*, 2008; *Rundel et al.*, 2009]. Automated minirhizotrons (AMR) were added to the study in 2008 and 2010 to track the dynamics of individual hyphae [*Allen et al.*, 2007; *Rundel et al.*, 2009; *Allen and Kitajima*, 2013]. We used four automated AMRs (Rhizosystems Inc. ®, Idyllwild, CA) to monitor hyphal growth at least once every 24 h since January of 2010. The frame size was 13 mm × 9 mm for the CMR, and 3.10 mm × 2.26 mm for the AMR. Images collected with CMR and AMR were digitized using ROOTFLY version 2 to measure length and diameter of fine roots, rhizomorphs, and hyphae (http://www.ces.clemson.edu/~stb/rootfly/). Approximately 90,000 CMR images and 7,300 AMR images were examined for the study. Relative length was calculated by dividing the length at time t by the maximum length over the entire year for each observed area.

[11] Eddy covariance observations of CO_2 and water vapor exchange were collected at the site beginning in 2006 [*Fellows and Goulden*, 2013; *Goulden et al.*, 2012]. The eddy flux tower footprint included the transect used for the sap flow and belowground observations.

[12] Twigs of dominant tree species, well and creek water, and soil samples were collected during the wet and dry seasons. Samples were sealed in vials and frozen within a few hours for storage. Water was subsequently extracted in the laboratory by cryogenic vacuum distillation. Isotopic signatures of δD and $\delta^{18}O$ were measured by mass spectroscopy (inductively coupled plasma (ICP)-MS, Agilent™ 7500ce, Agilent™ Technologies, U.S. (http://ccb.ucr.edu/firms.html)). The range of observed $\delta^{18}O$ was much smaller and its variation was relatively greater than δD (~$10^0/_{00}$ versus ~$50^0/_{00}$), and so we focused our analysis on δD. Data are reported in conventional delta notation, defined as the per mil ($^0/_{00}$) deviation from SMOW (Vienna standard mean ocean water):

$$\delta \mathrm{d}D = \left(R_{\mathrm{sample}} - R_{\mathrm{SMOW}}\right)/R_{\mathrm{SMOW}} * 1000,$$

where R_{sample} and R_{SMOW} are the $D/^2$H ratios in the samples and the SMOW standard, respectively. δD and $\delta^{18}O$ measurements had a precision of ±2%.

[13] The climate data are available at http://cens.jamesreserve.edu/jrcensweb/GUI/start.php. The belowground and sap flow data are available at http://ccb.ucr.edu/amarssdata.html. The minirhizotron images are available at http://cens.jamesreserve.edu/rootview/. The eddy covariance data are available at http://www.ess.uci.edu/~california/.

2.3. Model Description

[14] Observed and measured fluxes are shown in Figure 1, and optimized variables and constants taken from the literature are listed in Table 1. All fluxes (both observed and estimated) are presented on a ground area basis. The HYDRUS model is briefly described below.

[15] Soil water transport is governed by the Richards equation:

$$\partial\theta/\partial t = \partial/\partial z\,\{K(h) * \partial h/\partial z\} - S_{\mathrm{uptake}} + S_{\mathrm{HL}}, \qquad (1)$$

where θ (−) is soil water content, h (L)is the water pressure head, t (T) is time, z (L) is depth, $K(h)$ (LT^{-1}) is the hydraulic conductivity, S_{uptake} (LT^{-1}) is the plant water uptake rate, and S_{HL} (LT^{-1}) is the hydraulic lift rate. James Reserve has shallow (~2 m) sandy loam soil. Boundary conditions are the atmospheric flux at the upper boundary and a zero gradient at the bottom.

Table 1. Variables and Constants Used in the HYDRUS-1D Model

Labels	Dimensions	Variables	Values
a	cm^{-1}	Exponential space distribution of CO2 production.	Optimized
a_{ex}	(−)	Extinction coefficient for sunlight.	0.39
Alpha	cm^{-1}	Parameter a in the soil water retention, assuming van Genuchten-type curve.	0.075
b_1	$W\,cm^{-1}\,K^{-1}$	Coefficient b1 in the expression for the thermal conductivity function.	1.47E + 16
b_2	$W\,cm^{-1}\,K^{-1}$	Coefficient b2 in the expression for the thermal conductivity function.	−1.55E + 17
b_3	$W\,cm^{-1}\,K^{-1}$	Coefficient b3 in the expression for the thermal conductivity function.	3.17E + 17
c_a	(−)	Volumetric concentrations of CO_2 in gas phase.	
C_n	$J\,cm^{-3}\,K^{-1}$	Volumetric heat capacity of the solid phase.	1.43E + 14
C_o	$J\,cm^{-3}\,K^{-1}$	Volumetric heat capacity of organic matter.	1.87E + 14
C_p	$J\,cm^{-3}\,K^{-1}$	Volumetric heat capacity of the soil.	
Critical pressure head	cm	Value of the pressure head below which CO_2 production by soil microorganisms ceases.	−1.00E − 06
c_w	(−)	Volumetric concentrations of CO_2 in liquid phase.	
C_w	$J\,cm^{-3}\,K^{-1}$	Volumetric heat capacity of the liquid phase.	3.12E + 14
D_a	$cm^2\,d^{-1}$	Effective soil matrix diffusion coefficient of CO_2 in the gas phase.	13737.6
Dispersivity	cm	Longitudinal dispersivity for carbon dioxide.	1.5
D_l	cm	Longitudinal thermal dispersivity.	5
D_w	$cm^2\,d^{-1}$	Effective soil matrix dispersion coefficient of CO_2 in the dissolved phase	1.529
E_a^{root}	J	Activation energy of a CO_2 production of fine root and mycorrhizal fungi.	Optimized
E_a^{s}	J	Activation energy of a CO_2 production of soil microorganisms.	Optimized
f_h	(−)	Limiting factor for S_{HL} due to water pressure head difference.	
f_t	(−)	Limiting factor for S_{HL} due to time variation.	
f_t^0	(−)	Constant term for the limiting factor for S_{HL} due to time variation.	Optimized
g_i	(−)	Limiting factor for CO_2 production for each component.	
h	cm	Water pressure head.	
h_r	cm	Residual water pressure head for soil.	
h_{sat}	cm	Saturated water pressure head for soil.	
i	(−)	Denotes component, either soil or roots.	
K_{corr}	(−)	Scaling factor from FAO standard evapotranspiration to the one for the forest.	Optimized
K_s	$cm\,d^{-1}$	Saturated hydraulic conductivity.	Optimized
l	(−)	Tortuosity parameter in the soil water retention, assuming van Genuchten-type curve.	0.5
LAI	(−)	Leaf area index.	Observed
Michaelis' constant	(−)	Michaelis constant of CO_2 production by soil microorganisms.	0.19
Michaelis' constant	(−)	Michaelis constant for CO_2 production by plant roots.	0.14
n	(−)	Parameter n in the soil water retention, assuming Van Genuchten type curve.	1.89
Optimal pressure head	cm	Value of the pressure head for which CO_2 production by soil microorganisms is at the optimal level.	−1.00E − 03
Org	(−)	Volume fraction of organic matter in soil.	0
P	d^{-1}	CO_2 production.	
P_0	(−)	The exponent in the root water uptake response function associated with water stress, assuming van Genuchten-type curve.	3
P_{50}	cm	Root water uptake response function associated with water stress.	−800
PET	$cm\,d^{-1}$	Potential evapotranspiration for forest.	
PET^0	$cm\,d^{-1}$	FAO standard potential evapotranspiration.	
q	$cm\,d^{-1}$	Water flux.	
q_a	$cm\,d^{-1}$	Soil air flux.	
q_w	$cm\,d^{-1}$	Soil water flux.	
R		Gas constant.	
$R(z)$	(−)	Root density distribution function for temperate coniferous forests [*Jackson et al.*, 1996].	Observed
Sc_w	d^{-1}	CO_2 removed by the plant water uptake.	
S_{HL_0}	$cm\,d^{-1}$	Daily ground water hydraulically lifted from the weathered bedrock layer.	
S_{HL}	$cm\,d^{-1}$	Optimal daily ground water hydraulically lifted from the weathered bedrock layer.	Optimized
Solid	(−)	Volume fraction of solid phase in soil.	0.59
S_{uptake}	$cm\,d^{-1}$	Daily plant water uptake from the soil.	
t	day	Time.	
T	K	Soil temperature.	
z	cm	Soil depth from the soil surface.	
α	(−)	Limiting factor due to water stress for plant water uptake.	
θ	(−)	Soil water content.	
θ_w	(−)	Soil water content.	
θ_8	(−)	Soil water content at 8 cm depth in soil.	Observed
θ_a	(−)	Volumetric air content.	
$\theta_{crit,\ root}$	(−)	Critical soil water content for roots.	Optimized
θ_r	(−)	Residual soil water content for soil.	0.065
θ_s	(−)	Saturated soil water content for soil.	0.41
λ		Coefficient of the apparent thermal conductivity of the soil.	
γ_{root}^0	$cm\,d^{-1}$	Optimal CO_2 production by roots/mycorrhizae.	Optimized
γ_s^0	$cm\,d^{-1}$	Optimal CO_2 production by soil.	Optimized

[16] S_{uptake} at depth z is given by *Feddes et al*. [1978]:

$$S_{\text{uptake}}(z) = a * R(z) * \text{PET}, \quad (2)$$

where α ($0 < \alpha < 1$, $(-)$) is the water stress response function, $R(z)$ $(-)$ is the root density reported for temperate coniferous forests [*Jackson et al*., 1996] at depth z and was assumed to be independent of time; PET (LT^{-1}) is the forest-specific potential evapotranspiration. We assumed α was a van Genuchten-type function, which is an S-shaped curve that increases nonlinearly from 0 to 1 with increasing hydraulic potential. PET is related to Food and Agriculture Organization (FAO) standard PET (PET^0) by

$$\text{PET} = K_{\text{corr}} * \text{PET}^0 \lim_{x \to \infty}, \quad (3)$$

where K_{corr} $(-)$ is a correction factor for scaling from the PET^0 of the standard crop to a forest. PET^0 is given by the Penman equation and is a function of meteorological conditions and leaf area index (LAI, $(-)$). LAI was interpolated at a daily time step from satellite observations (https://lpdaac.usgs.gov/products/modis_products_table/mcd15a2, downloaded from the NASA Land Processes Distributed Active Archive Center, U.S. Geological Survey/Earth Resources Observation, and Science (EROS) Center, Sioux Falls, South Dakota).

[17] Several models of hydraulic lift exist [*Ryel et al*., 2002; *Zheng and Wang*, 2007; *Amenu and Kumar*, 2008; *Siqueira et al*., 2008], but we are unaware of previous efforts to incorporate hydraulic lift into HYDRUS. We added hydraulic lift into HYDRUS by assuming roots access water in the weathered bedrock and redistribute it throughout the rooting profile. This assumption was based on the patterns of moisture redistribution previously reported for California oak stands [*Querejeta et al*., 2007]. We incorporated hydraulic lift using the following simplifying rules.

[18] 1. Hydraulic lift takes place once every 24 h at midnight.

[19] 2. Deep moisture in the bedrock moves through roots, rhizomorphs, and hyphae to each soil layer based on the corresponding hydraulic potential difference. The bedrock is assumed to remain at "field capacity" year around. The roots, rhizomorphs, and hyphae are in the cracks and soil pockets of the bedrock.

[20] 3. The water storage capacity in fine roots, rhizomorphs, and hyphae is assumed to be zero.

[21] 4. The uplifted deep moisture is released and redistributed in proportion to the corresponding hydraulic potential difference and the fine root density, $R(z)$.

[22] 5. The soil temperature in each layer is adjusted at midnight by assuming the temperature of redistributed water is the same as the soil temperature at the bottom (2 m) of soil column.

[23] 6. Plant may reabsorb moisture according to equations (2) and (3) over the subsequent 24 h.

[24] 7. Plants are unable to withdraw moisture from extremely dry soil layers; the water content in dry layers reaches a residual value and water extraction from the layer ceases.

[25] These simplifications were intended to strike a balance between representing the full complexity of nature and producing a tractable model. For example, the first assumption —spontaneous redistribution of hydraulic lift moisture— was necessary to incorporate hydraulic lift into the stand alone HYDRUS model. Likewise, *Bleby et al*. [2010] used sap flow sensors in coarse lateral and deep roots to show that downward moisture redistribution through roots can occur after rain, whereas we ignored this possibility because monsoonal summer precipitation is rare in Southern California and the downward movement of water through roots is expected to occur infrequently.

[26] Hydraulic lift (upward water transfer) was expressed as

$$S_{\text{HL}}(z) = f_h * f_t * R(z) * S_{\text{HL}}{}^o, \quad (4)$$

where $S_{\text{HL}}(z)$ is the hydraulic lift rate at depth z, f_h ($0 < f_h < 1$, $(-)$) is a limiting factor due to the water potential difference between the soil and weathered bedrock, f_t is a limiting factor that accounts for seasonal hyphal biomass variation, and $S_{\text{HL}}{}^{\text{o}}$ (LT^{-1}) is the optimal hydraulic lift rate, which is constant. S_{HL} is the actual hydraulic lift water, which varies with depth and time due to the three factors, f_h , f_t , and $R(z)$. f_h at depth z is expressed as a linear function of water pressure head, h,

$$f_h(z) = (h_{\text{sat}} - h(z))/(h_{\text{sat}} - h_r), \quad (5)$$

where h_r and h_{sat} are the residual and saturated water pressure heads of the soil layer. This formulation is similar to that used for plant water uptake [*Feddes et al*., 1978].

[27] Our minirhizotron observation revealed that root/rhizomorph mass was relatively constant over the year but hyphal biomass increased during winter and decreased in late spring and early summer coincident with soil drying and warming. We therefore defined f_t as a limiting factor that accounts for seasonal variation of root, rhizomorph, and hyphae biomass. f_t $(-)$ was represented as a ramp function of soil water content at 0.08 m depth (θ_8),

$$\begin{aligned} &f_t = f_t{}^0, \text{if } \theta_8 < \theta_r, \\ &f_t = (\theta_8 - \theta_r)/(\theta_{\text{crit,root}} - \theta_r) * (1 - f_t{}^0) + f_t{}^0, \text{if } \theta_r < \theta_8 < \theta_{\text{crit,root}}, \\ &f_t = 1, \text{if } \theta_{\text{crit,root}} < \theta_8 < \theta_{\text{sat}}, \end{aligned} \quad (6)$$

where f_t^0 is a constant, and θ_r ,θ_{sat}, and $\theta_{\text{crit, root}}$ are residual, saturated, and critical soil water contents, respectively. For simplicity, f_t was assumed to be uniform throughout the soil column and h_8 was used as a proxy for the water potential of the entire soil column.

[28] Heat transport is described by

$$C_p(\theta) * \partial T_s/\partial z = \partial/\partial z[\lambda(\theta) * \partial T_s/\partial z] - C_w * q * \partial T_s/\partial z, \quad (7)$$

where $\lambda(\theta)$ is the coefficient of the apparent thermal conductivity of the soil and $C_p(\theta)$ and C_w are the volumetric heat capacities of the soil and the liquid phase, respectively, and q is the water flux density, which is determined by equation (1). The upper boundary condition is the extrapolated daily average soil temperature at the soil surface. The lower boundary condition is a zero gradient.

[29] CO_2 transport is described by

$$\begin{aligned} \partial/\partial t[c_a\theta_a + c_w\theta_w] = {} & \partial/\partial z[\theta_a D_a \partial c_a/\partial z] + \partial/\partial z[\theta_w D_w \partial c_w/\partial z] \\ & - \partial/\partial z[q_a c_a] - \partial/\partial z[q_w c_w] - Sc_w + P, \end{aligned} \quad (8)$$

where c_w $(-)$ and c_a $(-)$ are the volumetric concentrations of CO_2 in the dissolved and gas phases, D_a ($L^2\,T^{-1}$) is the effective soil matrix diffusion coefficient of CO_2 in the gas phase, D_w ($L^2\,T^{-1}$) is the effective soil matrix dispersion coefficient of CO_2 in the dissolved phase, q_a (LT^{-1}) is the soil air flux, q_w (LT^{-1}) is the soil water flux, θ_w $(-)$ is the soil water content and θ_a $(-)$ is the volumetric air content, Sc_w is the CO_2 removed by the plant water uptake, and P is the CO_2 production/sink term [*Šimůnek and Suarez*, 1993; *Suarez and Šimůnek*, 1993]. P is a sum of root and soil CO_2 production

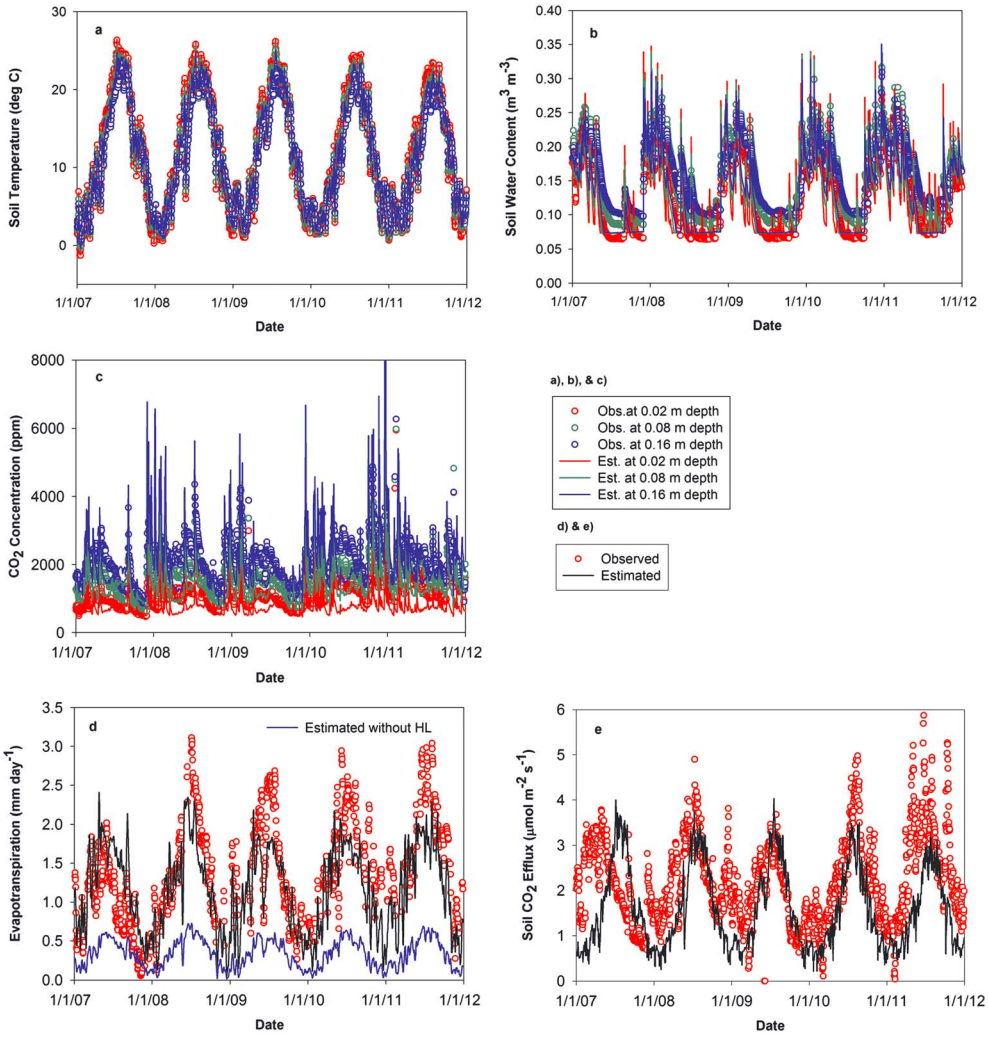

Figure 2. Daily trends of observed and estimated (a) soil temperature at three depths, (b) soil water content at three depths, (c) CO_2 concentration at three depths, (d) evapotranspiration (ET), and (e) soil CO_2 efflux. Observations are shown as open circles and estimates as solid lines. Modeled evapotranspiration (ET) without hydraulic lift is also shown in solid blue line in Figure 2d. ETs are shown as 7 day moving averages to reduce noise.

(distinguished by i). The CO_2 production for each component is the product of the optimal CO_2 production (γ_i^0) and the limiting factors (g_i), which are functions of z, θ, T_s, c_a, and t:

$$P = \sum_i \{R_i(z) * g_i(T) * g_i(c_a) * g_i(h) * g_i(t) * \gamma_i^0\}, \quad (9)$$

where, $R_i(z)$ (L^{-1}) is an exponential function describing root density; $g_i(T_s)$ (−) is an Arrhenius function (b*exp($-E_a/RT_s$), where E_a is an activation energy) describing the temperature sensitivity of CO_2 production; $g_i(c_a)$ (−) is a Michaelis-Menton function describing the effect of oxygen availability; $g_i(h)$ (−) is a Feddes function (also see equation (5)) [*Feddes et al.*, 1978] describing the effect of soil moisture on CO_2 production; γ_i^0 is the optimal CO_2 production for each component. For soil, $g_i(t)$ was assumed to be constant throughout the year (= 1). For roots, we used f_t for seasonal variation of root mass (equation (6)).

[30] We divided the soil column (2 m deep) into 100 layers and numerically solved the three differential equations (equations (1), (7), and (8)) on a daily basis. The model was calibrated using observed data for 2009 to optimize the 10 parameters in Table 1 by minimizing the negative log likelihood of the sum of squared errors, SS:

$$SS = \{y_i(\text{obs}) - y_i(\text{est})\}^2, \quad (10)$$

where y_i(obs) and y_i(est) are the observed and estimated values for soil CO_2 efflux, soil water content (θ), soil temperature (T_s), soil CO_2 concentration (C_{CO2}) at three depths, and evapotranspiration. Observed sap flow density was not used to calibrate the model but was used to compare with the pattern of the estimated transpiration rate (we lacked the detailed information of stand structure required to scale sap flow density to the stand level). We used MATLAB (R2011b, function fminsearch, http://www.mathworks.com/help/optim/ug/fminsearch.html) to optimize the model.

[31] We examined the effect of removing hydraulic lift from the model by optimizing for seven unknown parameters without equations (4) through (6), and then comparing the results with the output for the full model optimized for all

Table 2. Regression Results of Observed and Estimated Soil Temperature, Soil Water Content, CO_2 Concentration, Whole-Forest Evapotranspiration, and Soil CO_2 Efflux

Category	Constant	Slope	R^2
Soil temperature at 0.02 m	−0.0188	1.0008	0.9999
Soil temperature at 0.08 m	−0.2634	1.0637	0.9985
Soil temperature at 0.16 cm	−0.5664	1.0894	0.9979
Soil water content at 0.02 m	0.0155	0.8457	0.6368
Soil water content at 0.08 m	−0.0121	0.8990	0.7299
Soil water content at 0.16 m	−0.0472	1.1513	0.7408
CO_2 concentration at 0.02 m	0.0004	0.3270	0.1136
CO_2 concentration at 0.08 m	0.0005	0.6325	0.1543
CO_2 concentration at 0.16 m	0.0005	0.7778	0.2073
Evapotranspiration	0.0628	0.5065	0.5063
Soil CO_2 efflux	0.5411	0.4616	0.2549

10 unknowns. We tested the models against observed data for 2007, 2008, 2010, and 2011. We ran a linear regression between estimated and observed values and calculated the correlation and regression coefficients.

[32] We investigated the effect of spatial variation of the optimized parameters by separately optimizing the model for each observational node using soil temperature, soil moisture, soil CO_2 concentration at three depths, soil CO_2 efflux, and eddy covariance based evapotranspiration in 2007 (a total of nine nodes; we did not consider node #7 due to a high rate of missing data). The average, standard error (SE), and coefficient of variations (CV) were calculated for each unknown parameter. Rooting depth, root density, $R(z)$, biomass variation of fine roots/hyphae, f_t, were assumed to be the same for all nodes.

[33] The mass balance of water of the soil column was calculated as

$$\begin{aligned}\text{change in storage} = {} & \text{precipitation} + \text{hydraulic lift} \\ & - (\text{evaporation} + \text{transpiration}) \\ & + (\text{capillary rise or drain}),\end{aligned} \tag{11}$$

where change in storage is the water content increase or decrease in the soil column. Capillary rise (positive value) is the upward movement and drain (negative value) is the downward movement of moisture caused by the hydraulic potential difference between bedrock and soil column. We ignored horizontal water redistribution because of the gentle local slope. The local precipitation measurements are made near ground level, which minimizes the effect of canopy interception on the water balance.

3. Results

[34] The evapotranspiration predicted using HYDRUS without hydraulic lift was only one fifth that observed by eddy covariance (Figure 2d), implying that a representation of deep moisture access is crucial for modeling the local hydrology. We therefore added a parameterization of hydraulic lift to HYDRUS, as described in section 2. The resulting model did a better job of matching the observations (Figure 2 and Table 2). Soil temperature was in excellent agreement with the observed values (slope = 1.000–1.089, $R^2 > 0.998$, Figure 2a). Soil water content at 0.02 and 0.08 m was slightly underestimated (slope = 0.846 and 0.889, Figure 2b), while water content at 0.16 m was slightly overestimated (slope = 1.151). Evapotranspiration was still underestimated despite the inclusion of hydraulic lift (slope = 0.507, Figure 2d), though the predictions of evapotranspiration were much better than those made by the model without hydraulic lift (slope = 0.178). The degree of underestimation varied from year to year; the underestimation was greatest in 2008 (slope = 0.539) and least in 2007 (slope = 0.870).

[35] Deciduous *Quercus kelloggii* (California black oak) began to leaf out and transpire each year around day of year (DOY) 150 (30 May; Figure 3). Black oak leaf out was complete by the end of June and sap flow reached a maximum within 30 days. Black oak sap flow remained high (at least 80% of peak) for ~120 days before declining rapidly with leaf senescence from DOY 270 and 300 (October). The evergreen *Pinus ponderosa* and *P. lambertiana* transpired year-round, though the rates were suppressed and barely detectable on rainy, snowy, or cloudy days. Pine transpiration reached a maximum in May from DOY 120 to 150. Transpiration by

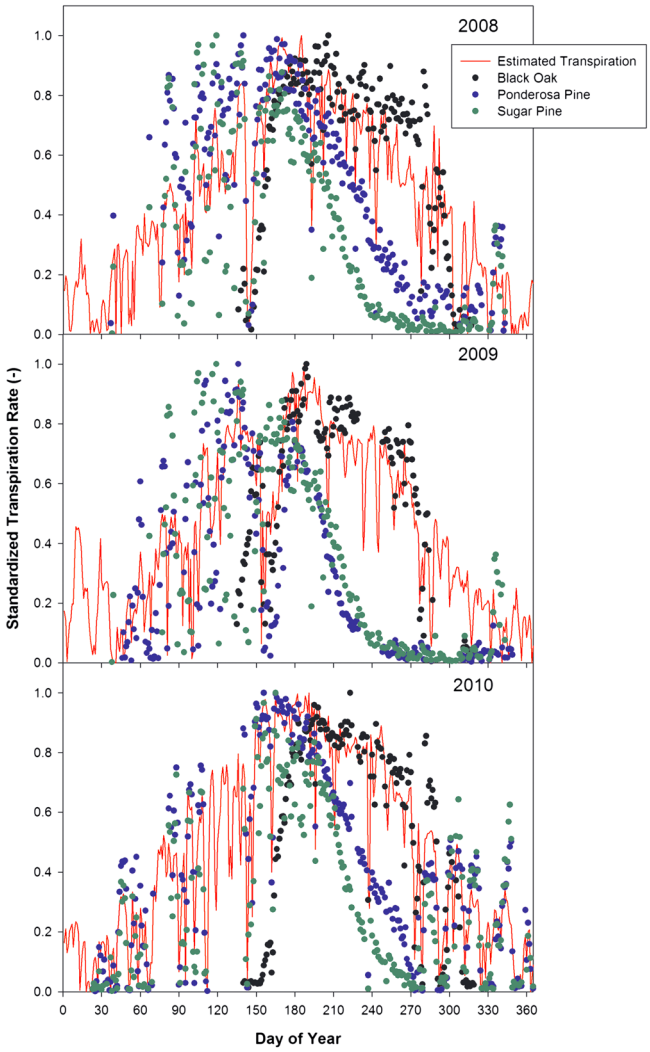

Figure 3. Comparison of estimated (solid red line) and observed transpiration for black oak (solid black circle), ponderosa pine (solid blue circle), and sugar pine (solid green circle). For comparison purpose, separate plots are shown for each year and all rates are standardized by dividing the daily rate by the maximum value of each year.

Table 3. Spatial Variation of Unknown Parameters Used in the Model Using Observed Data in Year 2007[a]

Node ID	K_{cor}	S_{HL}^{0}	γ_s^0	γ_{root}^0	a	E_a^s	E_a^{root}	K_s
1	0.1581	62.0123	0.2063	0.3801	0.3933	7791	5759	85.69
2	0.2409	67.6150	0.1221	0.4296	1.8154	7789	3260	88.03
3	0.1375	68.9840	0.1577	0.3032	0.9605	10300	2262	47.61
4	0.2851	67.7389	0.2780	0.4197	0.4491	7962	3839	56.84
5	0.1872	67.4219	0.1384	0.2641	0.7374	9765	3326	35.35
6	0.1628	68.9938	0.1924	0.1823	0.6656	10029	5149	75.05
8	0.2135	50.7938	0.1460	0.0981	0.6719	1106	5297	168.65
9	0.1610	59.5905	0.1328	0.1569	0.6170	8538	4361	75.79
10	0.2068	51.5112	0.1414	0.1406	0.4693	2255	4754	203.18
Average	0.1948	62.7402	0.1683	0.2639	0.7533	7282	4223	92.91
SE	0.0156	2.4382	0.0165	0.0421	0.1447	1111	380	18.73
CV	0.2410	0.1166	0.2946	0.4786	0.5762	0.4575	0.2699	0.6047

[a]Refer to the parameter list in Table 1 for symbols.

both pine species decreased slowly during the summer drought from DOY 180 to 270, while black oak transpiration remained high. Sugar pine transpiration declined more rapidly in summer than did ponderosa pine, at least in 2008 and 2010.

[36] The model underestimated soil CO_2 concentration at three depths and predictability was poor (slope = 0.327–0.778, R^2 = 0.114–0.207, Figure 2c). Soil CO_2 efflux was also underestimated (slope = 0.503, R^2 = 0.352, Figure 2e). These results are likely linked; low predictions of CO_2 concentration led to low predictions of soil CO_2 efflux.

[37] The optimized parameters were spatially variable, except for optimal uplift (S_{HL}^{o} in equation (4) and Table 3). This can be explained by the patchiness of trees, canopy coverage, under growth, and roots/hyphae. Factors affecting CO_2 production (a, exponential special distribution of CO_2 production, optimal production, γ_i^0, and activation energy E_a in equation (9)) also had large spatial variation, which may be related to spatial variation of microbial activity [*Klironomos et al.*, 1999]. The high spatial variation of saturated hydraulic conductivity (K_s) estimated by HYDRUS reflected variable soil properties across the transect. The soil under closed canopy was sandy loam with a comparatively high organic content; the soil under open canopy was sandier and had a lower organic content.

[38] The model indicated that hydraulic lift averaged ~28 mm month^{-1} in July and August and was negligible during the wet months, following the potential evapotranspiration trend (Figure 4a). Estimated evapotranspiration was the greatest in July, when the air temperature was the highest (Figure 4b). Estimated capillary rise was almost constant (~15 mm month^{-1}) between June and November. The ratio of hydraulic lift moisture to evapotranspiration peaked in August (~0.60, Figure 4c), and the ratio of capillary rise to evapotranspiration increased from June through November. Evapotranspiration exceeded the combined quantity of hydraulic lift and capillary rise during March through August, resulting in a gradual and continuous depletion of soil water. Precipitation, hydraulic lift, and capillary rise replenished dried soil in October and November. The annual quantity of hydraulically lifted moisture was ~112 mm yr^{-1}; the annual capillary rise was ~83 mm yr^{-1}. These findings indicate that both hydraulic lift and capillary rise contribute to evapotranspiration during dry months.

[39] Preliminary model runs showed that the addition of f_t in equation (6) did not substantially improve the model, and so f_t was set to 1 in the final analysis. Mycorrhizal fungi (both arbuscular and ectotrophic) and fine roots are interconnected and inseparable. Mycorrhizal fungi are not explicitly represented in the HYDRUS model; we incorpo-

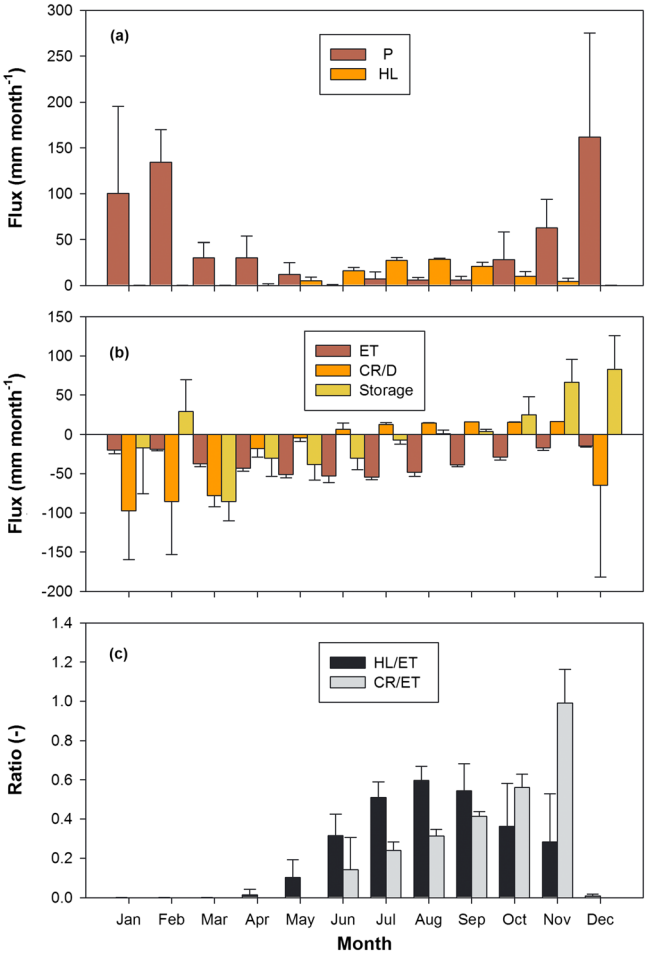

Figure 4. (a) Seasonal patterns of precipitation (P) and hydraulic lift (HL); (b), evapotranspiration (ET), capillary rise/drain (CR/D), and change in storage by month; (c) the ratios of hydraulically lifted moisture to ET (solid black bar) and capillary rise (solid gray bar) to ET. All fluxes except precipitation are estimated from the model. Error bars show 95% confidence interval for 2007 to 2011.

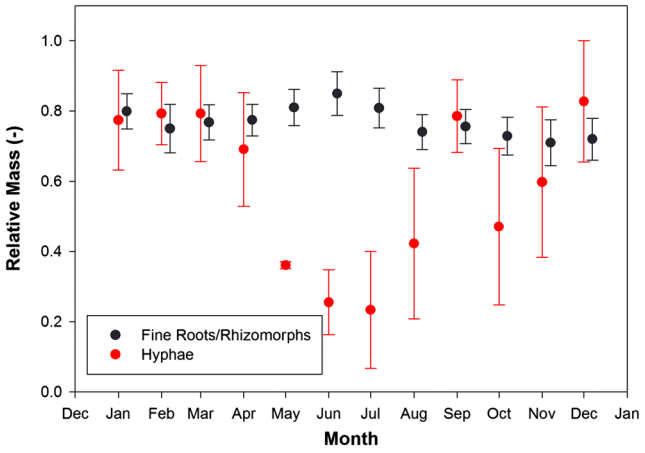

Figure 5. Relative mass of fine roots/rhizomorphs observed with 10 conventional minirhizotrons during 2005 to 2011 (black circle), and relative hyphal mass observed with four automated minirhizotrons in 2011 (red circle). Averages are shown as solid circles with error bars indicating 1 SE of spatial variation.

rated them by simply expanding the definition of roots to include the lumped root/fungi complex. Observed fine-root mass varied little over the year (Figure 5). A previous study showed that fine root production rate was greatest in late spring, coincident with warming and the occurrence of moist soil [*Kitajima et al.*, 2010]. The observed hyphal mass remained high during the winter and gradually decreased in late spring and summer coincident with warmer soil temperature. Hyphal lengths were lowest in late summer and fall coincident with drought. Hyphal length increased rapidly in November with the onset of the wet season.

[40] The isotopic composition of water collected during the wet season from individuals of the low-stature shrub *Eriogonum wrightii* was not significantly different from shallow soil water and significantly enriched with ^{2}H relative to groundwater (well, creek, and spring water, Figure 6a). In contrast, the composition of water collected from larger plants, including incense cedar, canyon live oak, and manzanita, was not significantly different from groundwater and less enriched than soil water. Tissue water collected during the dry season was more enriched than that collected during the wet season (Figure 6b). Water collected from *E. wrightii* during the summer was significantly enriched relative to groundwater and not significantly different from shallow soil water. Dry season water from incense cedar, interior live oak, sugar pine, and manzanita was not significantly different from groundwater and significantly less enriched than soil water. The isotopic composition of black oak samples collected during the winter were more enriched than soil

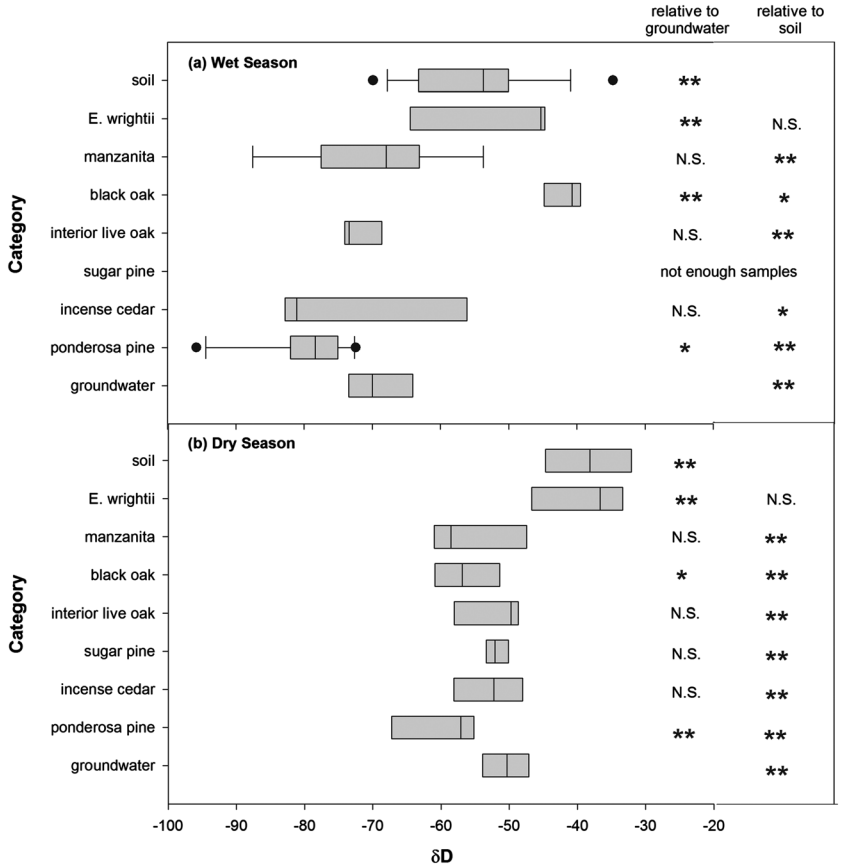

Figure 6. Comparison of δD values of various plant species, soil, and groundwater (creek, spring, and well) (a) during the wet season and (b) during the dry season. Comparisons marked with double asterisks were significantly at $p < 0.01$; those marked with a single asterisk were significantly different at $p < 0.05$; those marked with "N.S." were not significantly different.

water, though it is important to note that these samples were collected when the trees lacked leaves.

4. Discussion

[41] The comparison of HYDRUS with and without hydraulic lift demonstrated the need to consider deep moisture when modeling montane forest evapotranspiration. Adding hydraulic lift to HYDRUS closed much of the gap between modeled and observed evapotranspiration though some discrepancy remained. Much of the remaining difference may have been driven by the year-to-year variation of bedrock moisture. The year 2007 was one of the driest years in the last century, and it is likely that our assumption of a constant and ample source of deep moisture was violated during 2007 [*Fellows and Goulden*, 2013]. Further model refinement and new observational data are needed to track the year-to-year availability of moisture in the weathered bedrock. An additional source of uncertainty is the determination of potential evapotranspiration and subsequent calculation of actual evapotranspiration. Uncertainty in the eddy flux measurements could also contribute to the remaining mismatch between modeled and observed evapotranspiration.

[42] Plant access to deep moisture may be mediated by three mechanisms: capillary rise, deep root uptake and direct transfer to the canopy, and hydraulic redistribution. We were unable to fully explain the observations without including hydraulic redistribution in the model. Excluding hydraulic lift by resetting f_h, f_t, and $R(z)$ in equation (4) resulted in predictions that were poorer than those made when hydraulic lift was enabled. Similarly, a model based solely on deep root uptake and direct transfer to the canopy would have underestimated the water content of the soil during the summer; hydraulic lift is necessary to prevent excessive drying in the near-surface soil. *Ryel et al*. [2002] used a plant water uptake model to show that transpiration is very sensitive to root distribution; a more uniform root distribution led to a greater transpiration rate with and without hydraulic lift. We found that root density distribution had little effect on how well the model fit the observed data, and we could not fully explain the observed transpiration rate by changing root distribution alone. Hydraulic redistribution appears to play an important role in the hydrology of our site, though capillary rise and direct transfer to the canopy are also important; all three mechanisms contribute to deep moisture access.

[43] The species level observations of sap flow and water isotopes are generally consistent with the whole-ecosystem observations and model results. Whole-forest measured and modeled evapotranspiration was lowest before DOY 60, increased gradually with spring warming, reached a maximum around DOY 180, and declined in the late summer. Whole-forest evapotranspiration reflects the sum of all tree species as well as surface evaporation, and the seasonal patterns of evapotranspiration were in agreement with the combined patterns observed by sap flow. Hence, the winter rates of evapotranspiration appear to be attributable mainly to transpiration by the pines, the early summer evapotranspiration peak appears to reflect simultaneous high rates of transpiration by most of the species of trees; the evapotranspiration reduction during the late summer appears to reflect a decline in activity by the pines.

[44] The trees are deeply rooted and appear to access water in the weathered bedrock year-round, as predicted by the model. The small shrub *E. wrightii* with shallow roots apparently acquires most of its water from the surface soil. Ponderosa pine and black oak xylem water were significantly less enriched than the groundwater during both wet and dry seasons, suggesting that the roots of both species reach deeper in weathered bedrock than the other trees species. An interspecific difference in access to deep moisture was supported by the sap flow measurements, which showed sugar pine transpiration declines comparatively early in the dry season, ponderosa pine declines later in the dry season, and black oak transpiration appears largely decoupled from moisture availability and more tightly controlled by phenological shifts that may be associated with cold temperatures.

[45] Moisture from the weathered bedrock appears important for tree and shrub survival at the site. The combined quantity of hydraulically lifted moisture and capillary rise averaged 196 mm yr^{-1} from 2007 to 2011, which is ~1/3 of the mean precipitation during this period (578 mm yr^{-1}). Deep moisture presumably also contributes to the persistence of fine root/hyphal biomass during the summer drought, which we observed with the minirhizotrons. This conclusion is supported by *Querejeta et al*. [2007, 2009], who found that hydraulic redistribution facilitates the survival of both ectomycorrhizal roots and hyphae during extreme dry seasons.

[46] The model included a representation of soil CO_2 production. The rate of respiration by roots and associated mycorrhizae was 3.5 mm d^{-1} (γ_i^0 in equation (9)), and the rate of respiration by heterotrophic organisms was 2.2 mm d^{-1}, implying ~61% of soil respiration was generated by autotrophs. The Q_{10}s were 2.9 for heterotrophic respiration and 2.0 for roots; these values are within the range reported in the literature [*Burton et al*., 2002].

[47] The model's underestimation of CO_2 efflux from the soil was a direct consequence of the underestimation of soil CO_2 concentration. Part of this discrepancy may have reflected the importance of the duff layer of fallen leaves and twigs at several nodes. The model did not include a representation of the duff layer. An additional source of uncertainty is the tortuosity factor used to calculate CO_2 diffusion. HYDRUS follows Millington and Quirk [*Millington and Quirk*, 1961], whereas measurements at the site using concentration profiles and soil respiration chambers gave results that were closer to Marshall [*Marshall*, 1959]. Additionally, the optimized parameters related to CO_2 production, including soil and root CO_2 production (γ_i^0), depth sensitivity (a), and temperature sensitivity (E_a^s), were spatially variable; additional work is needed to improve the representation of soil CO_2 concentration and efflux in models.

5. Conclusions and Implications

[48] Our findings provide strong evidence that the trees at our site depend on deep moisture to support year-round gas exchange. We combined modeling and isotopic measurements to show that deep water access and hydraulic lift play important roles in semiarid forest hydrology. *Bales et al*. [2011] and *Goulden et al*. [2012] reported similar patterns for Sierra Nevada mixed coniferous forest. Likewise, *Ichii et al*. [2009] used satellite-based observations and an ecosystem model to infer that rooting depths in California,

especially in evergreen forest, are deeper than previously thought. Global climate models project an extended dry season and warmer temperatures by 2100. A critical question moving forward is whether warming and drying will limit summer production and carbon fixation, or whether access to deep water and hydraulic lift will allow many of the trees at our site to continue to avoid summer drought stress. Further refinements of the approach we describe above may be able to address this issue.

[49] **Acknowledgments.** The authors thank Jirka Šimůnek for invaluable advice on running HYDRUS-1D. Hai Vo, Renee Wang, Tim Mok, Stephanie Ngo, Kevin Choy, and Daniel Tran helped process the image data. Mike Taggart and Tom Unwin with Rhizosystems Inc. developed and maintained the automated minirhizotrons. This work was performed at the University of California Natural Reserve System James Reserve. Special thanks to Becca Fenwick and the management and workers at the James Reserve. This research was funded by the National Science Foundation (EF-0410408 and CRR-0120778) and the Department of Energy Terrestrial Ecosystem Sciences program (Project ID 0011182).

References

Aber, J. D., and C. A. Federer (1992), A generalized, lumped-parameter model of photosynthesis, evapotranspiration and net primary production in temperate and boreal forest ecosystems, *Oecologia*, *92*(4), 463–474, doi:10.1007/BF00317837.

Allen, M. F. (1991), *The Ecology of Mycorrhizae*, pp. 105, Cambridge University Press.

Allen, M. F. (2009), Bidirectional water flows through the soil-fungal-plant mycorrhizal continuum, *New Phytol.*, *182*(2), 290–293, doi:10.1111/j.1469-8137.2009.02815.x.

Allen, M. F., W. Swenson, J. I. Querejeta, L. M. Egerton-Warburton, and K. K. Treseder (2003), Ecology of mycorrhizae: A conceptual framework for complex interactions among plants and fungi, *Annu. Rev. Phytopathol.*, *41*(1), 271–303, doi:10.1146/annurev.phyto.41.052002.095518.

Allen, M. F., et al. (2007), Soil sensor technology: Life within a pixel, *BioScience*, *57*(10), 859–867.

Allen, M. F., and K. Kitajima (2013), In situ high frequency observations of mycorrhizas, *New Phytol.*, *200*, 222–228, doi:10.1111/nph.12363.

Amenu, G. G., and P. Kumar (2008), A model for hydraulic redistribution incorporating coupled soil-root moisture transport, *Hydrol. Earth Syst. Sci. Discussions*, *12*(1), 55–74.

Amthor, J. S., et al. (2001), Boreal forest CO2 exchange and evapotranspiration predicted by nine ecosystem process models: Intermodel comparisons and relationships to field measurements, *J. Geophys. Res.*, *106*(D24), 33,623–33,648, doi:10.1029/2000JD900850.

Bales, R. C., J. W. Hopmans, A. T. O'Geen, M. Meadows, P. C. Hartsough, P. Kirchner, C. T. Hunsaker, and D. Beaudette (2011), Soil moisture response to snowmelt and rainfall in a Sierra Nevada mixed-conifer forest, *Vadose Zone J.*, *10*(3), 786–799, doi:10.2136/vzj2011.0001.

Bleby, T. M., A. J. Mcelrone, and R. B. Jackson (2010), Water uptake and hydraulic redistribution across large woody root systems to 20 m depth, *Plant Cell Environ.*, *33*(12), 2132–2148, doi:10.1111/j.1365-3040.2010.02212.x.

Bornyasz, M. A., R. C. Graham, and M. F. Allen (2005), Ectomycorrhizae in a soil-weathered granitic bedrock regolith: Linking matrix resources to plants, *Geoderma*, *126*(1–2), 141–160, doi:10.1016/j.geoderma.2004.11.023.

Braswell, B. H., W. J. Sacks, E. Linder, and D. S. Schimel (2005), Estimating diurnal to annual ecosystem parameters by synthesis of a carbon flux model with eddy covariance net ecosystem exchange observations, *Global Change Biol.*, *11*(2), 335–355, doi:10.1111/j.1365-2486.2005.00897.x.

Burgess, S. S., M. A. Adams, N. C. Turner, and C. K. Ong (1998), The redistribution of soil water by tree root systems, *Oecologia*, *115*(3), 306–311.

Burton, A. J., K. S. Pregitzer, R. W. Ruess, R. L. Hendrick, and M. F. Allen (2002), Root respiration in North American forests: Effects of nitrogen concentration and temperature across biomes, *Oecologia*, *131*(4), 559–568, doi:10.1007/s00442-002-0931-7.

Cayan, D., E. Maurer, M. Dettinger, M. Tyree, and K. Hayhoe (2008), Climate change scenarios for the California region, *Clim. Change*, *87*, 21–42, doi:10.1007/s10584-007-9377-6.

Egerton-Warburton, L. M., R. C. Graham, and K. R. Hubbert (2003), Spatial variability in mycorrhizal hyphae and nutrient and water availability in a soil-weathered bedrock profile, *Plant Soil*, *249*(2), 331–342, doi:10.1023/A:1022860432113.

Egerton-Warburton, L. M., J. I. Querejeta, and M. F. Allen (2007), Common mycorrhizal networks provide a potential pathway for the transfer of hydraulically lifted water between plants, *J. Exp. Bot.*, *58*(6), 1473–1483, doi:10.1093/jxb/erm009.

Egerton-Warburton, L. M., J. I. Querejeta, and M. F. Allen (2008), Efflux of hydraulically lifted water from mycorrhizal fungal hyphae during imposed drought, *Plant Signal. Behav.*, *3*(1), 68–71, doi:10.4161/psb.3.1.4924.

Feddes, R. A., P. J. Kowalik, and H. Zaradny (1978), *Simulation of Field Water Use and Crop Yield*, Wageningen, Centre for Agricultural Pub. and Documentation.

Fellows, A., and M. L. Goulden (2013), Controls on gross production by a semiarid forest growing near its warm and dry ecotonal limit, *Agric. For. Meteorol.*, *169*, 51–60.

Glenn, E. P., K. Morino, P. L. Nagler, R. S. Murray, S. Pearlstein, and K. R. Hultine (2012), Roles of saltcedar (Tamarix spp.) and capillary rise in salinizing a non-flooding terrace on a flow-regulated desert river, *J. Arid Environ.*, *79*, 56–65, doi:10.1016/j.jaridenv.2011.11.025.

Goulden, M. L., R. G. Anderson, R. C. Bales, A. E. Kelly, M. Meadows, and G. C. Winston (2012), Evapotranspiration along an elevation gradient in California's Sierra Nevada, *J. Geophys. Res.*, *117*, G03028, doi:10.1029/2012JG002027.

Graham, R. C., A. M. Rossi, and K. R. Hubbert (2010), Rock to regolith conversion: Producing hospitable substrates for terrestrial ecosystems, *GSA Today*, *20*, 4–9, doi:10.1130/GSAT57A.1.

Granier, A. (1987), Evaluation of transpiration in a Douglas-fir stand by means of sap flow measurements, *Tree Physiol.*, *3*(4), 309–320, doi:10.1093/treephys/3.4.309.

Hayhoe, K., et al. (2004), Emissions pathways, climate change, and impacts on California, *Proc. Natl. Acad. Sci. U.S.A.*, *101*(34), 12,422–12,427, doi:10.1073/pnas.0404500101.

Hubbert, K. R., J. L. Beyers, and R. C. Graham (2001), Roles of weathered bedrock and soil in seasonal water relations of Pinus Jeffreyi and Arctostaphylos patula, *Can. J. For. Res.*, *31*(11), 1947–1957, doi:10.1139/x01-136.

Ichii, K., W. Wang, H. Hashimoto, F. Yang, P. Votava, A. R. Michaelis, and R. R. Nemani (2009), Refinement of rooting depths using satellite-based evapotranspiration seasonality for ecosystem modeling in California, *Agric. For. Meteorol.*, *149*(11), 1907–1918, doi:10.1016/j.agrformet.2009.06.019.

Jackson, R. B., J. Canadell, J. R. Ehleringer, H. A. Mooney, O. E. Sala, and E. D. Schulze (1996), A global analysis of root distributions for terrestrial biomes, *Oecologia*, *108*(3), 389–411, doi:10.1007/BF00333714.

Kitajima, K., K. E. Anderson, and M. F. Allen (2010), Effect of soil temperature and soil water content on fine root turnover rate in a California mixed conifer ecosystem, *J. Geophys. Res.*, *115*, G04032, doi:10.1029/2009JG001210.

Klironomos, J. N., M. C. Rillig, and M. F. Allen (1999), Designing belowground field experiments with the help of semi-variance and power analyses, *Appl. Soil Ecol.*, *12*(3), 227–238, doi:10.1016/S0929-1393(99)00014-1.

Knohl, A., and D. D. Baldocchi (2008), Effects of diffuse radiation on canopy gas exchange processes in a forest ecosystem, *J. Geophys. Res.*, *113*, G02023, doi:10.1029/2007JG000663.

Kurz-Besson, C., et. al. (2006), Hydraulic lift in cork oak trees in a savannah-type Mediterranean ecosystem and its contribution to the local water balance, *Plant Soil*, *282*(1-2), 361–378, doi:10.1007/s11104-006-0005-4.

Lilleskov, E. A., T. D. Bruns, T. E. Dawson, and F. J. Camacho (2009), Water sources and controls on water-loss rates of epigeous ectomycorrhizal fungal sporocarps during summer drought, *New Phytol.*, *182*(2), 483–494, doi:10.1111/j.1469-8137.2009.02775.x.

Ludwig, F., T. E. Dawson, H. De Kroon, F. Berendse, and H. H. T. Prins (2003), Hydraulic lift in Acacia tortilis trees on an East African savanna, *Oecologia*, *134*, 293–300, doi:10.1007/s00442-002-1119-x.

Marshall, T. J. (1959), The diffusion of gases through porous media, *J. Soil Sci.*, *10*(1), 79–82, doi:10.1111/j.1365-2389.1959.tb00667.x.

Miller, G. R., X. Chen, D. Baldocchi, and Y. Rubin (2010), Groundwater uptake by woody vegetation in a Mediterranean oak savanna, *Water. Resour. Res.*, *46*, W10503, doi:10.1029/2009WR008902.

Millington, R. J., and J. P. Quirk (1961), Permeability of porous solids, *Trans. Faraday Soc.*, *57*, 1200–1207, doi:10.1039/tf9615701200.

Moreira, M. Z., F. G. Scholz, S. J. Bucci, L. S. Sternberg, G. Goldstein, F. C. Meinzer, and A. C. Franco (2003), Hydraulic lift in a neotropical savanna, *Functional Ecol.*, *17*(5), 573–581.

Nadezhdina, N., et al. (2010), Trees never rest: The multiple facets of hydraulic redistribution, *Ecohydrology*, *3*(4), 431–444, doi:10.1002/eco.148.

Orellana, F., P. Verma, S. P. Loheide II, and E. Daly (2012), Monitoring and modeling water-vegetation interactions in groundwater-dependent ecosystems, *Rev. Geophys.*, *50*, RG3003, doi:10.1029/2011RG000383.

Parton, W. J., et al. (1993), Observations and modeling of biomass and soil organic matter dynamics for the grassland biome worldwide, *Global Biogeochem. Cycles*, *7*(4), 785–809, doi:10.1029/93GB02042.

Parton, W. J., M. Hartman, D. Ojima, and D. Schimel (1998), DAYCENT and its land surface submodel: Description and testing, *Global Planet. Change*, *19*(1–4), 35–48, doi:10.1016/S0921-8181(98)00040-X.

Prieto, I., C. Armas, and F. I. Pugnaire (2012), Water release through plant roots: New insights into its consequences at the plant and ecosystem level, *New Phytol.*, *193*(4), 830–841, doi:10.1111/j.1469-8137.2011.04039.x.

Querejeta, J. I., L. M. Egerton-Warburton, and M. F. Allen (2007), Hydraulic lift may buffer rhizosphere hyphae against the negative effects of severe soil drying in a California oak savanna, *Soil Biol. Biochem.*, *39*(2), 409–417, doi:10.1016/j.soilbio.2006.08.008.

Querejeta, J., L. Egerton-Warburton, and M. Allen (2003), Direct nocturnal water transfer from oaks to their mycorrhizal symbionts during severe soil drying, *Oecologia*, *134*(1), 55–64, doi:10.1007/s00442-002-1078-2.

Querejeta, J., L. M. Egerton-Warburton, and M. F. Allen (2009), Topographic position modulates the mycorrhizal response of oak trees to interannual rainfall variability, *Ecology*, *90*(3), 649–662, doi:10.1890/07-1696.1.

Richards, J. H., and M. M. Caldwell (1987), Hydraulic lift: Substantial nocturnal water transport between soil layers by Artemisia tridentata roots, *Oecologia*, *73*(4), 486–489, doi:10.1007/BF00379405.

Ruess, R. W., R. L. Hendrick, A. J. Burton, K. S. Pregitzer, B. Sveinbjornssön, M. F. Allen, and G. E. Maurer (2003), Coupling fine root dynamics with ecosystem carbon cycling in black spruce forests of interior Alaska, *Ecol. Monogr.*, *73*(4), 643–662, doi:10.1890/02-4032.

Rundel, P. W., E. A. Graham, M. F. Allen, J. C. Fisher, and T. C. Harmon (2009), Environmental sensor networks in ecological research, *New Phytol.*, *182*(3), 589–607, doi:10.1111/j.1469-8137.2009.02811.x.

Ryel, R. J., M. M. Caldwell, C. K. Yoder, D. Or, and A. J. Leffler (2002), Hydraulic redistribution in a stand of Artemisia tridentata: Evaluation of benefits to transpiration assessed with a simulation model, *Oecologia*, *130*(2), 173–184, doi:10.1007/s004420100794.

Šimůnek, J., and D. L. Suarez (1993), Modeling of carbon dioxide transport and production in soil: 1. Model development, *Water Resour. Res.*, *29*(2), 487–497, doi:10.1029/92WR02225.

Simunek, J., M. T. Van Genuchten, and M. Sejna (2005), The HYDRUS-1D software package for simulating the one-dimensional movement of water, heat, and multiple solutes in variably-saturated media, University of California, Riverside, Research Reports, 240.

Siqueira, M., G. Katul, and A. Porporato (2008), Onset of water stress, hysteresis in plant conductance, and hydraulic lift: Scaling soil water dynamics from millimeters to meters, *Water Resour. Res.*, *44*, W01432, doi:10.1029/2007WR006094.

Suarez, D. L., and J. Šimůnek (1993), Modeling of carbon dioxide transport and production in soil: 2. Parameter selection, sensitivity analysis, and comparison of model predictions to field data, *Water Resour. Res.*, *29*(2), 499–513, doi:10.1029/92WR02226.

Tang, J., P. V. Bolstad, B. E. Ewers, A. R. Desai, K. J. Davis, and E. V. Carey (2006), Sap flux-upscaled canopy transpiration, stomatal conductance, and water use efficiency in an old growth forest in the Great Lakes region of the United States, *J. Geophys. Res.*, *111*, G02009, doi:10.1029/2005JG000083.

Vargas, R., and M. F. Allen (2008), Dynamics of fine root, fungal rhizomorphs, and soil respiration in a mixed temperate forest: Integrating sensors and observations, *Vadose Zone J.*, *7*(3), 1055–1064, doi:10.2136/vzj2007.0138.

Warren, J. M., J. R. Brooks, F. C. Meinzer, and J. L. Eberhart (2008), Hydraulic redistribution of water from Pinus ponderosa trees to seedlings: Evidence for an ectomycorrhizal pathway, *New Phytol.*, *178*, 382–394, doi:10.1111/j.1469-8137.2008.02377.x.

Warren, J. M., F. C. Meinzer, J. R. Brooks, J.-C. Domec, and R. Coulombe (2007), Hydraulic redistribution of soil water in two old-growth coniferous forests: Quantifying patterns and controls, *New Phytol.*, *173*(4), 753–765, doi:10.1111/j.1469-8137.2006.01963.x.

Witty, J. H., R. C. Graham, K. R. Hubbert, J. A. Doolittle, and J. A. Wald (2003), Contributions of water supply from the weathered bedrock zone to forest soil quality, *Geoderma*, *114*(3–4), 389–400, doi:10.1016/S0016-7061(03)00051-X.

Yin, J., M. H. Young, and Z. Yu (2008), Effects of paleoclimate and time-varying canopy structures on paleowater fluxes, *J. Geophys. Res.*, *113*, D06103, doi:10.1029/2007JD009010.

Yuan, F., T. Meixner, M. E. Fenn, and J. Šimůnek (2011), Impact of transient soil water simulation to estimated nitrogen leaching and emission at high- and low-deposition forest sites in Southern California, *J. Geophys. Res.*, *116*, G03040, doi:10.1029/2011JG001644.

Zheng, Z., and G. Wang (2007), Modeling the dynamic root water uptake and its hydrological impact at the Reserva Jaru site in Amazonia, *J. Geophys. Res.*, *112*, G04012, doi:10.1029/2007JG000413.